Journal of Assisted Reproduction and Genetics (2020) 37:1329–1339
https://doi.org/10.1007/s10815-020-01784-9

TECHNOLOGICAL INNOVATIONS

Whole-ovary decellularization generates an effective 3D bioscaffold for ovarian bioengineering

Georgia Pennarossa[1] · Matteo Ghiringhelli[1] · Fulvio Gandolfi[2] · Tiziana A. L. Brevini[1]

Received: 16 December 2019 / Accepted: 14 April 2020 / Published online: 2 May 2020

Abstract

Purpose To develop a new protocol for whole-ovary decellularization for the production of a 3D bioscaffold suitable for in vitro/ex vivo studies and for the reconstruction of a bioengineered ovary.

Methods Porcine ovaries were subjected to the decellularization process (DECELL; $n=20$) that involved a freeze-thaw cycle, followed by sequential incubations in 0.5% SDS for 3 h, 1% Triton X-100 for 9 h, and 2% deoxycholate for 12 h. Untreated ovaries were used as a control (CTR; $n=6$). Both groups were analyzed to evaluate cell and DNA removal as well as ECM preservation. DECELL bioscaffolds were assessed for cytotoxicity and cell homing ability.

Results DECELL ovaries maintained shape and homogeneity without any deformation, while their color turned from red to white. Histological staining and DNA quantification confirmed a decrease of 98.11% in DNA content, compared with the native tissue (CTR). Histochemical assessments demonstrated the preservation of intact ECM microarchitecture after the decellularization process. This was also confirmed by quantitative analysis of collagen, elastin, and GAG contents. DECELL bioscaffold showed no cytotoxic effects in co-culture and, when re-seeded with homologous fibroblasts, encouraged a rapid cell adhesion and migration, with repopulating cells increasing in number and aggregating in cluster-like structures, consistent with its ability to sustain cell adherence, proliferation, and differentiation.

Conclusion The protocol described allows for the generation of a 3D bioscaffold that may constitute a suitable model for ex vivo culture of ovarian cells and follicles, as well as a promising tool for the reconstruction of a bioengineered ovary.

Keywords 3D bioscaffold · Decellularization · Extracellular matrix · Porcine · Whole ovary

Introduction

Ovary dysfunction and premature ovarian failure (POF) represent the maiARG001784sn causes of infertility, with an alarming incidence of one out of 1000 women, under the age of 30, rising to 1.0–1.5% in women younger than 40 years [1, 2]. Patients affected are not able to undergo physiological cycles and/or release oocytes, nor they produce normal levels of hormones [3]. Infertility is currently considered a multiple medical and psychosocial challenge, since it is accompanied by severe menopause symptoms, such as osteoporosis, cardiovascular disease, autoimmune disorders, and depression [4]. Several potential causes have been identified, including viral infections, environmental factors, metabolic and autoimmune disorders, and genetic predisposition [2, 5, 6]. Furthermore, the recent advances in cancer therapy have significantly increased the number of tumor survivors who suffer from therapy-induced ovarian failure [7]. To date, several options to restore ovarian functions have been developed and used in clinics, including embryo and oocyte cryopreservation [8–15]. More recently, ovarian fragment or whole ovary preservation, followed by allogeneic transplantation into the patient, has been also proposed as a possible solution, with no issues related to rejection or need for immunosuppression [16–22]. However, since this procedure is largely devoted to cancer patients, the high risk of re-introduction of malignant cells poses a severe limit to its use in clinical practices [23–25]. It

✉ Tiziana A. L. Brevini
tiziana.brevini@unimi.it

[1] Laboratory of Biomedical Embryology, Department of Health, Animal Science and Food Safety and Center for Stem Cell Research, Università degli Studi di Milano, via Celoria 10, 20133 Milan, Italy

[2] Department of Agricultural and Environmental Sciences - Production, Landscape, Agroenergy and Center for Stem Cell Research, Università degli Studi di Milano, via Celoria 2, 20133 Milan, Italy

is therefore evident an urgent need for a safe and effective alternative to restore female fertility. In this perspective, bioengineered ovary reconstruction is one of the most promising strategies recently proposed. Currently, there is a growing interest on decellularization techniques, wherein living cells are removed from an organ to produce extracellular matrix (ECM)–based 3D bioscaffolds. In contrast to gel matrices previously used, these supports retain intact ECM structures that are able to recreate in vitro the complex in vivo milieu, facilitating the necessary interactions between cells and their surroundings and ensuring a correct cell growth, differentiation, and function [26]. These features make ECM-based bioscaffolds a predictive and reliable in vitro model for studying organ functions and pathologies, as well as a promising tool for drug testing and bioengineered organ reconstruction. Indeed, the absence of cells and the low immunogenicity of the decellularized ECM make it an ideal tool for allotransplantation [27]. To date, the use of decellularization processes has been reported in different organs, such as the heart [28], lung [29], liver [30], kidney [31], muscle [32], trachea [33], esophagus [34], urinary tissue [35], arteries [36], derma [26], and vagina [37]. However, limited studies have been performed in the reproductive system, and, more specifically, in the ovarian tissue [38, 39]. The first attempt was described in 2015, when decellularized ECM was successfully obtained from bovine ovaries, suggesting for the first time the possibility to preserve organ macro- and micro-structures, suitable for creating a supportive niche for ovarian cell growth [39]. Subsequently, similar protocols were applied to ovarian tissue fragments isolated from different species [40–43], while the decellularization of one entire ovary was limited to the bovine [39] and the mouse [43, 44]. In particular, the creation of a bioprosthetic organ able to re-establish ovarian hormonal activity in ovariectomized animals, leading to the generation of healthy offspring, was demonstrated in murine species [43, 44]. Implementation of this approach and its application to large animal models would increase the hopes of translating this technology to human patients. In the present study, we selected the porcine specie based on its anatomical and physiological similarities to the humans. We produced a whole ovary decellularized bioscaffold to be used as a reliable and predictive 3D model for in vitro studies of ovarian development, function, and pathology. We suggest that the generated scaffold may constitute a suitable niche for ex vivo culture of ovarian cells and follicles, as well as a promising tool for the reconstruction of a bioengineered ovary.

Materials and methods

All reagents were purchased from Sigma unless otherwise indicated.

Ovary collection

Ovaries were collected from gilts weighing approximately 120 kg at the local slaughterhouse and transported to the laboratory in cold sterile PBS. They were randomly allocated to the untreated control (CTR; $n = 6$) or to the decellularized treated (DECELL; $n = 23$) group. CTR samples were immediately fixed in 10% buffered formalin for histological evaluations or subjected to DNA quantification analysis. DECELL group ovaries were subjected to the decellularization process.

Decellularization process

Whole ovaries were removed from PBS, placed in 50-ml tubes (Sarstedt) and frozen at − 80 °C for at least 24 h. Entire organs were then thawed at 37 °C in a water bath for 30 min and treated with 0.5% sodium dodecyl sulfate (SDS; Bio-Rad) in deionized water (DI-H_2O) for 3 h, followed by an overnight incubation in 1% Triton X-100 in DI-H_2O. Samples were extensively washed in DI-H_2O for 9 h and, subsequently, immersed in 2% deoxycholate in DI-H_2O for 12 h. Lastly, decellularized whole ovaries were washed in DI-H_2O for 6 h with changes every 2 h. All steps were carried out using an orbital shaker at 200 rpm at room temperature. At the end of the procedure, 3 DECELL ovaries were subjected to SEM analysis. DNA content was analyzed in the remaining DECELL ovaries ($n = 20$) by cutting small pieces (10 fragments, ranging from 15 to 25 mg) from each of them. Subsequently, 8 out of 20 DECELL ovaries were fixed for histology, 4 were used for protein quantification studies, and 8 were subjected to in vitro studies ($n = 4$ for cytotoxicity assessment and $n = 4$ for re-seeding of bioscaffolds).

Scanning electron microscopy

Three DECELL ovaries were rinsed in deionized water to remove detergent residues and cut with a scalpel to expose regions of interest. Samples were fixed in 2.5% glutaraldehyde plus 4% paraformaldehyde aqueous solution at 4 °C overnight and, subsequently, gradually dehydrated via an increasing graded ethanol-water series up to 100% ethanol (30%, 70%, 80%, 90%, and 100%, 15 min each). Samples were then immersed respectively into 1:3, 1:1, and 3:1 hexamethyldisilazane (HMDS; Merck):ethanol for 20 min and 100% HMDS solution overnight to air-dry in a fume hood. They were mounted on aluminum foil covered with carbon tape, coated with a thin layer of gold (SEMPrep 2, Nanotech) and imaged using a LEO 1430 SEM (Zeiss) at 7 kV accelerating voltage.

Histological evaluations

Eight DECELL ovaries were fixed in 10% buffered formalin for 24 h at room temperature, dehydrated in graded alcohols, cleared with xylene, and embedded in paraffin. After dewaxing and re-hydration, serial microtome sections (5 µm thick) were stained with hematoxylin and eosin (H&E, Bio-Optica) to evaluate the general structural aspects of all samples. To confirm the efficient cell removal, sections were stained with 4′,6-diamidino-2-phenylindole (DAPI; Thermo Fisher Scientific).

ECM structures were qualitatively analyzed with Masson (Bio-Optica) and Mallory trichrome staining (Bio-Optica) for the detection of collagen and collagen/elastic fibers, respectively. Gomori's aldehyde-fuchsin (Bio-Optica) was used to detect elastic fibers alone, Alcian blue (pH 2.5; Bio-Optica) for total glycosaminoglycans (GAGs), and Alcian blue/periodic acid-Schiff (PAS) for distinguishing neutral from acid GAGs. For each staining, 10 sections were obtained from each DECELL ovary and 5–10 histological fields per section were evaluated. Specimens were observed under an Eclipse E600 microscope (Nikon) equipped with a digital camera (Nikon). Pictures were acquired with the NIS-Elements Software (Version 4.6; Nikon).

Cell density

Cell number was counted in 15 tissue sections obtained from 3 DECELL (5 sections for each) and 3 control ovaries (5 sections for each). In each section, 5 randomly selected fields at × 100 total magnification were analyzed. Cell density was evaluated per square millimeter. Pictures were taken with constant exposure parameters in order to be analyzed with the image analysis software ImageJ (http://rsbweb.nih.gov/ij/index.html), using the specific Cell Counter plugin. Briefly, threshold adjustments were applied on generated 8-bit black-and-white images. Images were then segmented with a thresholding algorithm to highlight areas occupied by the nuclei and remove the background. Data acquired were transformed in binary form. Size and circularity parameters were set, and nuclei were automatically counted.

DNA quantification

Ten fragments, ranging from 15 to 25 mg, were cut from all DECELL ovaries ($n = 20$). Fragment weights were annotated for the subsequent DNA content calculations. Genomic DNA was extracted with the PureLink® Genomic DNA Kit (Thermo Fisher Scientific), following the manufacturer's instructions. DNA concentration was assessed with NanoDrop 8000 (Thermo Fisher Scientific).

Collagen quantification

Biophysical active collagen content was analyzed in fragments obtained from 4 DECELL ovaries using the Insoluble Collagen Assay – Sircol™ kit (Tebu-bio SRL), according to the manufacturer's instructions. Briefly, 20 mg of wet sample was homogenized in 0.1 M HCl-pepsin solution. Fragmentation reagent was added and incubated for 3 h at 65 °C, vortexing every 30 min. Subsequently, Sircol dye reagent and collagen content were measured at a wavelength of 550 nm. The experiments were performed at least in triplicate.

Elastin quantification

Elastin was quantified in 4 DECELL ovaries using the Fastin Elastin Assay kit (Tebu-bio SRL). Samples were heated at 100 °C with 0.25 M oxalic acid for three 1-h periods, to solubilize the elastin. The latter was then precipitated for 15 min, centrifuged, and stained with Fastin dye reagent containing 5,10,15,20-tetraphenyl-21H,23H-porphine tetrasulfonate (TPPS) in a citrate-phosphate buffer for 90 min. Absorbances were read at 513 nm. The analyses were carried out at least in triplicate.

Glycosaminoglycan quantification

Sulfated GAG content was analyzed in 4 DECELL ovaries using the Glycosaminoglycan Assay Blyscan™ kit (Tebu-bio SRL), following the manufacturer's instructions. Briefly, 20 mg (wet weight) of each sample was digested in 1 ml of Papain extraction reagent for 3 h at 65 °C, occasionally vortexing. After centrifuge at 10,000*g* for 10 min, Blyscan dye (1, 9-dimethylmethylene blue) was added and incubated using a mechanical shaker for 30 min. GAG content was measured at 656 nm. The experiments were performed at least in triplicate.

Isolation and culture of porcine fibroblasts

Primary porcine skin fibroblast cultures were established from fresh biopsies. Fragments of tissue of approximately 2 mm^3 were transferred to a 0.1% pig gelatin pre-coated Petri dish (Sarstedt) and cultured in DMEM with 20% FBS (Thermo Fisher Scientific), 2 mM glutamine, and antibiotics. After 4 days, primary fibroblast cultures started to grow out of the tissue fragments which were carefully removed. Cells were cultured under standard conditions [45] and passaged twice a week in a 1:3 ratio.

Cytotoxicity assessment

3(4,5-Dimethylthiazole-2-yl)-2,5-diphenyltetrazolium-bromide (MTT, Roche) assay was performed on 4 DECELL

ovaries to determine the cytotoxicity of decellularized whole ovaries. Briefly, porcine fibroblasts were seeded onto flat-bottom 96-well plates at a concentration of 5×10^3 cells/ml (100 µl per well). After 24 h, DECELL ovaries were sterilized using 70% ethanol and 2% antibiotic solution in sterile H_2O for 30 min, extensively washed in PBS, and cut in halves with a scalpel to expose the regions of interest and accurately separate the cortex from the medulla. A total of 20 mg tissue obtained by mixing 10 mg of cortical and 10 mg of medullary region of each DECELL ovary was added to cells in triplicates and co-cultured for 1, 3, and 7 days. Ten microliters of MTT solution was then added to media and incubated for 4 h. Formazan salt crystals were dissolved in 100 µl of 10% SDS in 0.01 M HCl overnight. The optical density (OD) was measured at 550 nm. The same cell number seeded without decellularized whole-ovary fragments was used as control.

Re-seeding of bioscaffolds

Four DECELL ovaries were sterilized using 70% ethanol and 2% antibiotic solution in sterile H_2O for 30 min and extensively washed in PBS. Twelve scaffolds 7 mm in diameter and 1 mm thick were obtained from each ovary, using sharp scalpel. A total of 7×10^6 porcine fibroblasts were seeded onto scaffolds and cultured in 4-well multidishes (Nunc, Thermo Fisher Scientific) with 300 µl of standard culture medium [45]. Half medium volume was changed every 2 days. Seeded scaffolds were maintained in a 37 °C incubator with 5% CO_2. Culture was arrested for histological evaluations and DNA quantification after 24 h and 3 and 7 days.

Statistical analysis

Statistical analysis was performed using Student's *t* test or ANOVA with Tukey's post hoc (SPSS 19.1; IBM). At least three experiments were carried out for all analyses. Data were reported as mean ± standard deviation (SD). Differences of $p \leq 0.05$ were considered significant.

Results

Whole-ovary decellularization eliminates cellular components

Macroscopic observations during the decellularization process showed that ovaries maintained their shape and homogeneity without any deformation (Fig. 1a–c). However, their color turned from red to white, indicating changes in cellular components (Fig. 1a–c).

Both H&E and DAPI staining showed that the obtained bioscaffolds were devoid of cells. Indeed, H&E demonstrated the absence of basophilic staining in DECELL ovaries (Fig. 1e). In contrast, both the basophilic and eosinophilic staining were visible in CTR ovaries (Fig. 1d). DAPI and cell density results were consistent with those of H&E, confirming a significantly lower number of nuclei in DECELL tissues (Fig. 1g, h) compared with the untreated ones (CTR; Fig. 1f, h).

In agreement with this, DNA quantification showed a 98.11% decrease of the DNA content in DECELL ovaries compared with the native tissue (CTR). In particular, a content of 0.03 ± 0.01 µg DNA/mg of tissue was measured in DECELL vs. 1.59 ± 0.08 µg DNA/mg of tissue in CTR (Fig. 1i).

Whole-ovary decellularization preserves microarchitecture and ECM components

Scanning electron microscopy (SEM) assessment showed microarchitecture integrity of DECELL ovaries (Fig. 2a–h). Low magnification demonstrated successfully cell removal with cell-free preserved cavities and empty space where it once contained follicles, stromal cells, and blood vessels (Fig. 2a–c). Higher magnification images showed the ovarian surface epithelium in the cortical area (Fig. 2d) and revealed intact ECM framework and the maintenance of well-connected and oriented collagen fibers (Fig. 2e–h).

Histochemical assessments demonstrated the preservation of ECM after the decellularization process. In particular, both Masson (Fig. 3a, b) and Mallory trichrome staining (Fig. 3c, d) showed the persistence of collagen fibers after the decellularization process (Fig. 3b, d). Collagen displayed a comparable distribution between DECELL (Fig. 3b, d) and CTR tissues (Fig. 3a, c), showing a diffuse localization both in the cortex and in the medullary regions. These morphological observations were confirmed by collagen content analyses, where no significant differences were detected between CTR (52.8 ± 4.1 µg/mg of tissue) and treated (DECELL; 49.9 ± 5.7 µg/mg of tissue) groups (Fig. 3k). In parallel, Mallory trichrome staining (Fig. 3c, d) indicated the maintenance of elastic fibers (red magenta) after the decellularization process. This was also confirmed by Gomori's aldehyde-fuchsin staining demonstrating DECELL tissues displaying elastic fibers scattered throughout the ovary, especially concentrated near the vessels (Fig. 3f). A similar distribution was detected in untreated CTR ovaries (Fig. 3e). Furthermore, elastin quantification studies supported these results, showing comparable amount of elastin before (37.2 ± 1.5 µg/mg of tissue) and after (35.1 ± 1.7 µg/mg of tissue) the decellularization process (Fig. 3l). Alcian blue staining revealed GAG retention in DECELL tissues (Fig. 3h). This was also confirmed by quantitative analysis that displayed no significant reduction in total GAG content in DECELL ovaries (5.2 ± 0.4 µg/mg µg/mg of tissue) compared with CTR samples (5.7 ± 0.3 µg/mg of tissue; Fig. 3m). Accordingly, Alcian blue/PAS staining indicated

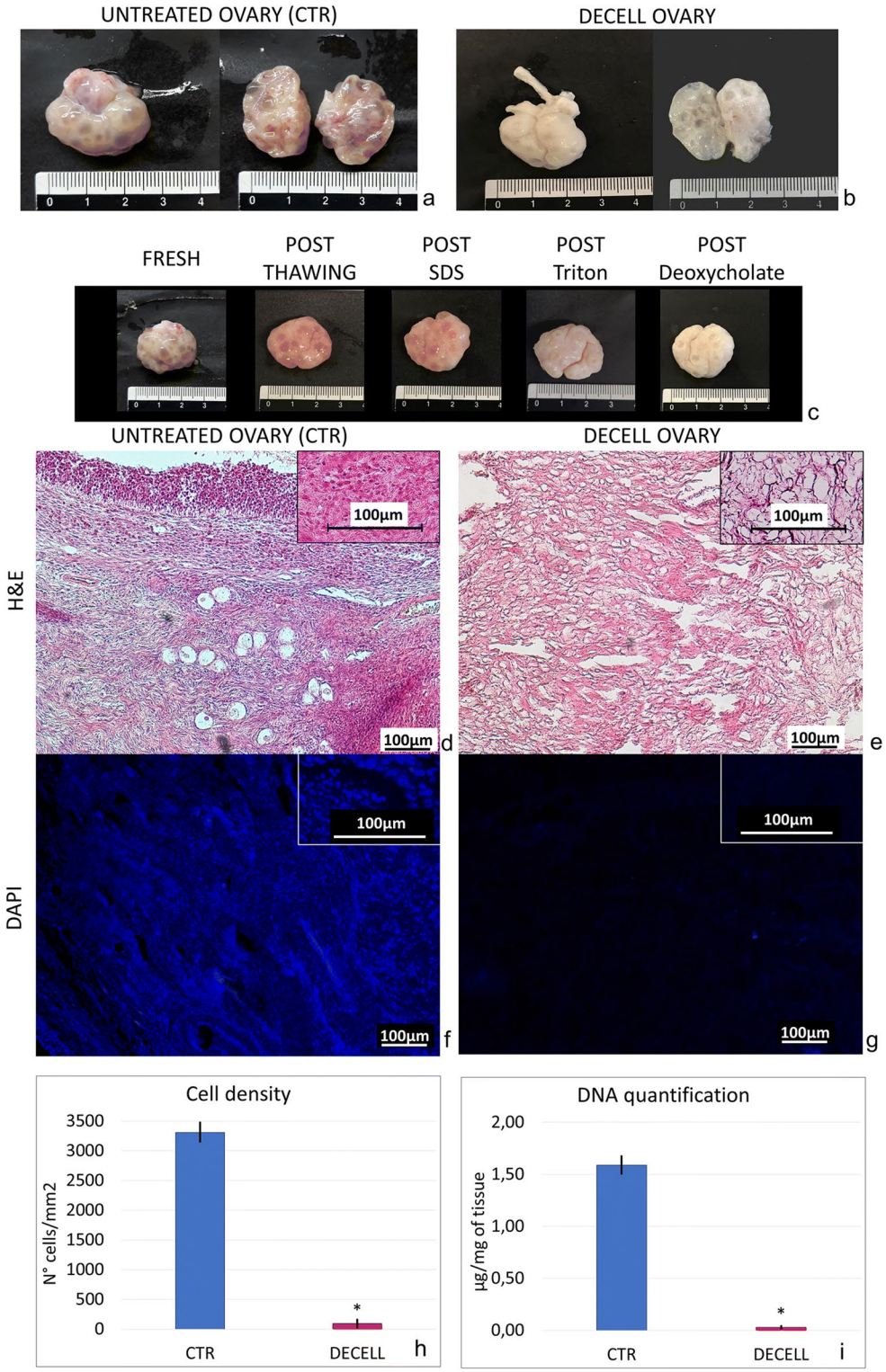

Fig. 1 Macro/microscopic evaluations and DNA quantification in untreated (CTR) and decellularized (DECELL) ovaries. **a**, **b** CTR and DECELL ovaries display comparable shapes and homogeneity, while their color turns from red (CTR; **a**) to white (DECELL; **b**). **c** Chronological macroscopic images illustrating the decellularization process. **d**, **e** Hematoxylin-eosin staining shows the presence of both basophilic (cell nuclei) and eosinophilic (cell cytoplasm and ECM) staining in untreated tissue (CTR; **d**), while cell nuclei and the related basophilic staining are absent in DECELL ovaries (**e**). **f**, **g** DAPI staining displays the presence of nuclei in CTR ovaries (**f**) and their disappearance after the decellularization process (DECELL; **g**). **h** Cell density demonstrates a significantly lower number of nuclei in DECELL tissues compared with that in the untreated ones (CTR). Data are expressed as the mean ± standard error of the mean (SEM), $*p<0.05$. **i** DNA quantification analysis showed a significant decrease in the DNA content of DECELL ovaries compared with that of the native tissue (CTR). Data are expressed as the mean ± standard error of the mean (SEM). $*p<0.05$

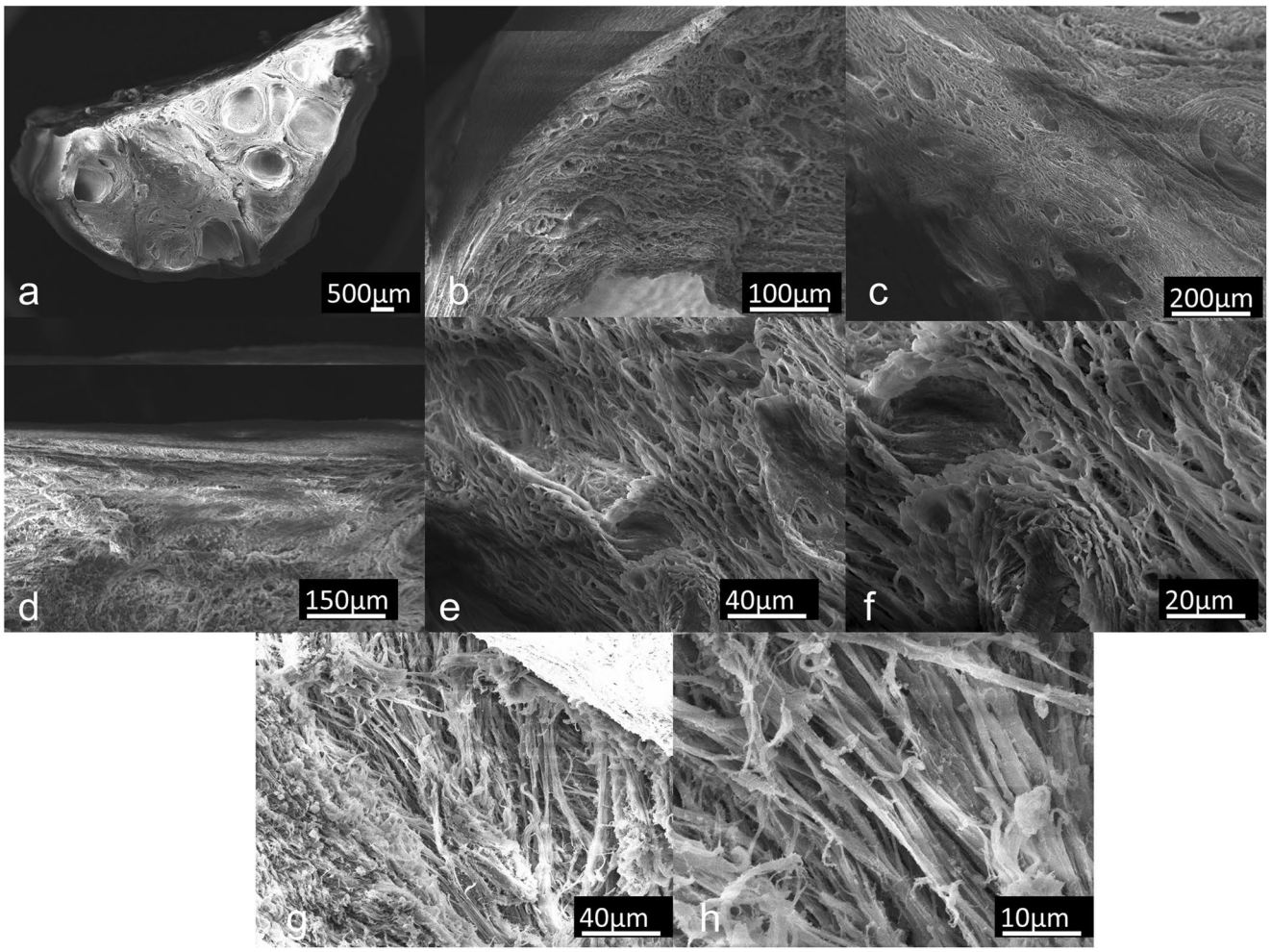

Fig. 2 Scanning electron microphotographs of decellularized (DECELL) ovaries. **a** Decellularized hemiovary section. **b**, **c** Efficient cell removal, preservation of 3D microarchitecture, and ECM integrity are revealed after the decellularization process. Porous structures once populated by different cell types and complex fiber network are visible. **d**–**h** The ovarian surface epithelium and well-organized collagen fibers within pore walls are distinguishable

comparable distribution of acid (Alcian blue, blue) and neutral (PAS, red magenta) GAGs between decellularized (Fig. 3j) and untreated tissue (Fig. 3i).

Decellularized ovarian tissue shows no cytotoxic effects

MTT assay demonstrated no cytotoxic effects exerted by DECELL tissue. In particular, no significant differences in OD values were detected between cells co-cultured with DECELL and those of control (CTR; Fig. 4a). The two groups displayed comparable viability at day 1 and day 3 of culture (Fig. 4a). In addition, even protracted exposure (7 days) indicated the absence of cytotoxic response and confirmed the efficient removal of the detergent compounds used during decellularization (Fig. 4a).

Decellularized ovarian tissue supports cell adhesion

Re-seeded porcine fibroblasts rapidly migrated into the bioscaffolds, adhering and colonizing the ECM within 24 h (Fig. 4c, day 1). During the subsequent days of culture, an increasing number of cells and the formation of cluster-like structures were visible (Fig. 4c, day 3) and steadily maintained up to 7 days (Fig. 4c, day 7), when culture was arrested.

These observations were supported by H&E and DAPI staining, which demonstrated the presence of cells into the bioscaffolds already after 24 h of co-culture (Fig. 4d–f, day 1). Interestingly, cell number increased in the following days (Fig. 4d–f, Day3) and were steadily maintained up to 7 days (Fig. 4d–f, day 7).

In agreement with all morphological data, DNA quantification analyses demonstrated an increasing DNA content during the entire length of the experiments. In particular, 0.25 ± 0.02, 1.18 ± 0.07, and 1.39 ± 0.08 µg of DNA/mg of

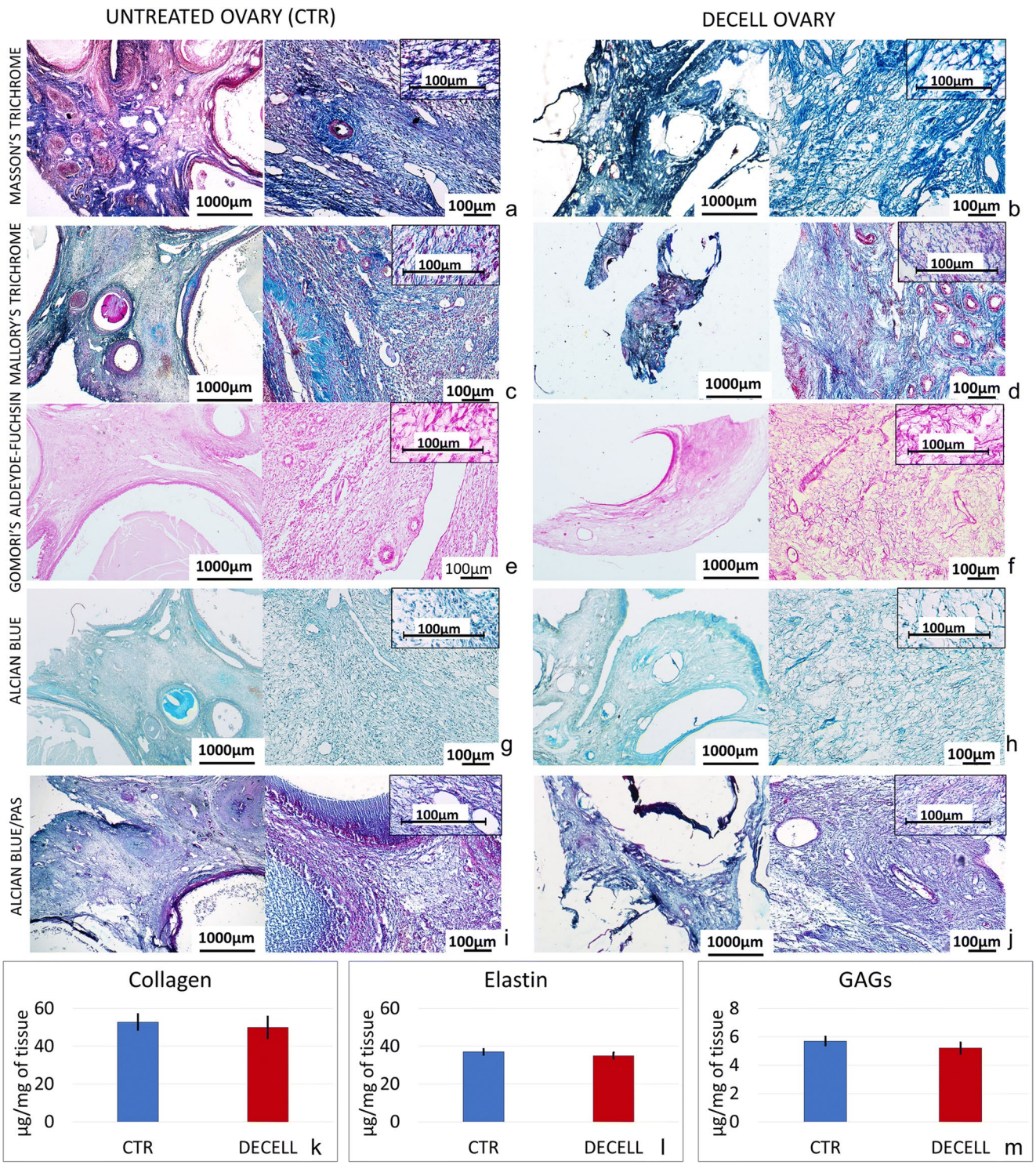

Fig. 3 ECM microarchitecture and composition in untreated (CTR) and decellularized (DECELL) ovaries. **a**, **b** Masson's trichrome staining shows the persistence of collagen fibers (blue) and their comparable distribution between CTR (**a**) and DECELL (**b**) tissues. **c**, **d** Mallory's trichrome staining demonstrates the maintenance of intact collagen (blue) and elastic fibers (pink) after the decellularization process (DECELL; **d**). **e**, **f** Gomori's aldehyde-fuchsin staining confirms that DECELL tissues (**f**) retain elastic fibers scattered throughout the ovary, similarly to CTR ovaries (**e**). **g**, **h** Alcian blue staining reveals GAG retention in DECELL tissues (**h**). **i**, **j** Alcian blue/PAS staining indicates comparable distribution of neutral (magenta) and acid (blue) GAGs between DECELL (**j**) and CTR tissue (**i**). **k** Collagen content analysis demonstrates no significant differences between CTR and DECELL groups. Data are expressed as the mean ± standard error of the mean (SEM) ($p > 0.05$). **l** Elastin quantification shows comparable amount of the protein before (CTR) and after the decellularization process (DECELL). Data are expressed as the mean ± standard error of the mean (SEM) ($p > 0.05$). **m** Total GAG analysis contents display no significant reductions in DECELL ovaries compared with CTR ones. Data are expressed as the mean ± standard error of the mean (SEM) ($p > 0.05$)

tissue were detected after 1, 3, and 7 days of culture, respectively (Fig. 4g).

Discussion

Assisted reproduction techniques and hormone replacement therapies presently used for clinical treatments do not provide a definitive solution for female fertility restoration, and safe and effective alternatives are mandatory. Ovarian bioengineering may represent a promising approach and is currently the focus of several researches with the final goal of obtaining structures that could be used in patients, from childhood to adult age, for initiating puberty, restoring endocrine dysfunctions, or, more in general, re-establishing reproductive ability. The use of decellularized tissues that maintain an intact ECM with which cells interact and integrate according to their specific requirements has been recently proposed [46, 47]. In the present study, we describe for the first time a new protocol to successfully decellularize whole ovaries obtained from a large mammal, selecting the pig as a model, based on its anatomical and physiological similarities to the human. We propose a four-step procedure that involves a freeze-thaw cycle, followed by sequential incubations with SDS, Triton X-100, and deoxycholate, which are generally considered strong, intermediate, and weak reagents, respectively [26].

At the end of the decellularization process, macroscopic evaluations revealed the maintenance of ovarian shape and homogeneity, without any deformation, with color changing from red to white and suggesting the occurrence of significant reduction in the cellular components. A similar color variation was previously reported by Hassanpour [42], who applied a decellularization process to human ovarian fragments that resulted in a drastic decrease in cell content. This was confirmed by our histological evaluations that demonstrated the absence of basophilic and DAPI staining, indicating a significant decrease in cell nuclei. In addition, these morphological observations were further corroborated by the DNA quantification analysis that showed a decrement of 98.11% in DNA content after decellularization. Previous experiments carried out on ovarian tissue fragments reported a DNA residual ranging from 15% [39] to 0.33% [41]. Altogether, these results demonstrate the effectiveness of the protocol proposed in the present manuscript and, more in details, suggest that the correct use of a freeze-thaw cycle, in combination with specific detergents, allows for the obtainment of whole-ovary decellularized bioscaffolds, with an intact macrostructure and only 1.89% of DNA content.

It is important to remember that a fundamental aspect in the decellularization protocol is the balance between an effective removal of the cellular compartment and the maintenance of the original ECM microstructures, including fibers and macromolecules. In this context, the use of SDS is still debated and needs to be further clarified. Indeed, while previous studies showed SDS ability to successfully eliminate cells and create DECELL ovary scaffolds able to restore hormone function [39, 48], home MSCs [43], or human follicles [40], other authors suggested a detrimental effect of this detergent, with damages to structural proteins, such as collagen fibers [49, 50] and GAGs [51]. In the present study, scanning electron microscopy analysis confirms an efficient cell removal and demonstrates microarchitecture integrity of DECELL ovaries. In particular, preserved cavities and empty spaces, once containing follicles, stromal cells, and blood vessels, were visible together with intact ECM framework with well-connected and oriented collagen fibers. In addition, histochemical analysis demonstrated the preservation of intact collagen and elastic fibers as well as the persistence of an unaltered distribution of neutral and acid GAGs in decellularized whole ovaries. These morphological observations were also confirmed by quantitative analysis of the related proteins, which revealed no significant changes between control (CTR) and treated (DECELL) groups for collagen, elastin, and GAG content. These results are very encouraging and in agreement with a recent work by Henning et al., where almost all matrisome proteins obtained from porcine decellularized ovaries were clearly read and mapped across the cortical and medullary compartments by relative abundance [52]. A possible explanation for the optima protein preservation could be found in the reduction of SDS incubation period/tissue size ratio. Indeed, studies currently present in literature describe the occurrence of ECM damages when similar experimental conditions were applied to smaller ovarian fragments [40, 41, 43], suggesting for the need to identify a distinct balance between time of exposure to the detergent and tissue weight. Similarly, detergent remnants within the decellularized bioscaffolds

Fig. 4 Cytotoxicity and re-seeding of decellularized ovarian tissue. **a** MTT assay demonstrates no significant differences in OD values between cells co-cultured with DECELL and those of control (CTR) at the different time points analyzed. Data are expressed as the mean ± standard error of the mean (SEM) ($p > 0.05$). **b** Images illustrating the scaffold before re-seeding. **c** Re-seeded porcine fibroblasts rapidly migrate into the bioscaffolds within 24 h (day 1). An increasing number of cells and the formation of cluster-like structures are visible at day 3 and steadily maintained at day 7. **d** H&E staining demonstrates the presence of cells into the bioscaffolds after 24 h of co-culture (day 1), with an increment during the following days (day 3 and day 7). **e** DAPI staining confirms the positivity for nuclei from 24 h onward. **f** Cell density shows bioscaffold re-population after 24 h (day 1), with a higher cell number at day 3 and day 7. Data are expressed as the mean ± standard error of the mean (SEM). Different superscripts denote significant differences ($p < 0.05$). **g** DNA quantification analysis demonstrates the presence of cells at day 1, which increases in number at day 3 and is steadily maintained at day 7. Data are expressed as the mean ± standard error of the mean (SEM). Different superscripts denote significant differences ($p < 0.05$)

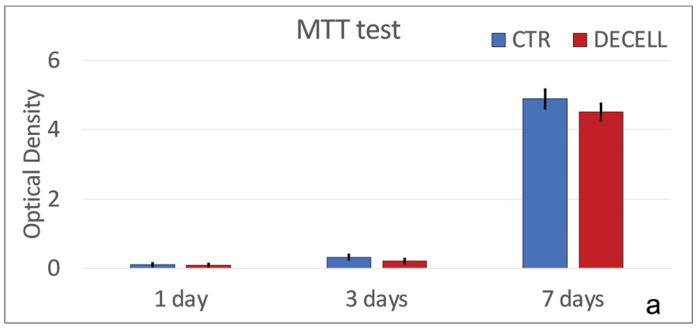

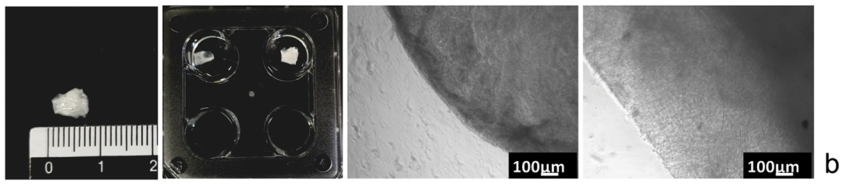

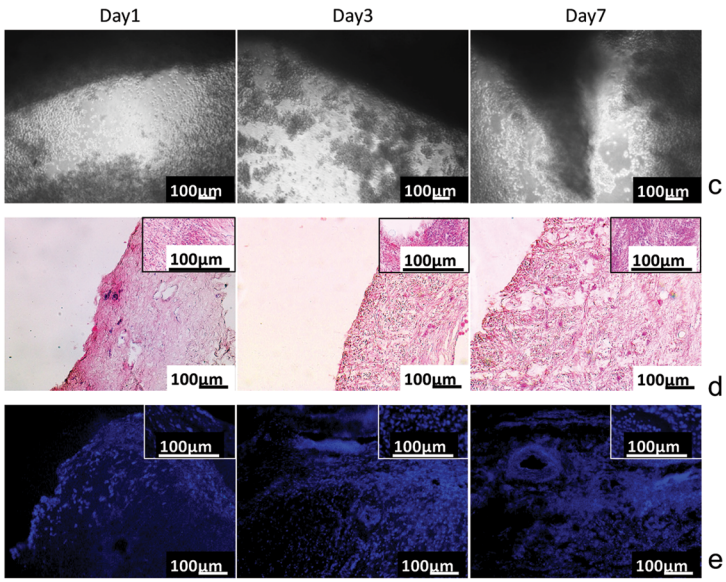

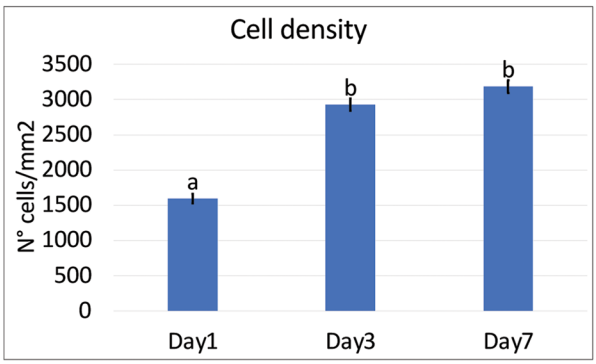

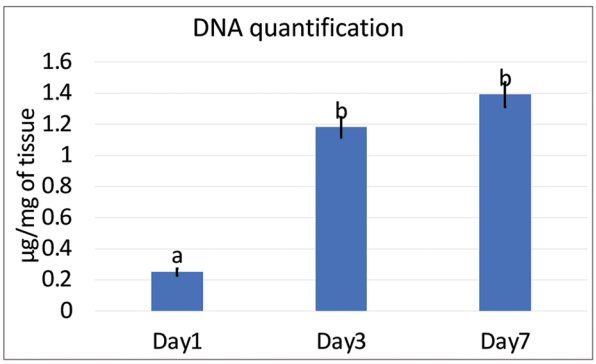

are a crucial point and may impair the subsequent recellularization and biocompatibility, both in vitro and in vivo [53]. Cytotoxicity, evaluated by MTT, revealed no significant differences in OD values between cells co-cultured with decellularized whole-ovary fragments and those of the CTR group. These results are very encouraging and allow us to consider any toxic effect exerted by the bioscaffold in culture as very unlikely. Indeed, its re-seeding with porcine fibroblasts demonstrated a rapid cell adhesion and migration within the first 24 h, with repopulating cells increasing in number and aggregating in cluster-like structures. Interestingly, histological and DNA content analysis

demonstrated a steady maintenance of cell distribution and homing within the scaffold for as long as 7 days, when culture was arrested, suggesting the regenerative potential of the whole-ovary bioscaffold here described and implying its ability to sustain cell adherence and proliferation. These evidences appear even more interesting in light of previous observations by Laronda et al. who suggest the use of personalized medicine techniques in the future of a safe artificial ovary for human use [54]. In particular, the cell type selected for our re-seeding experiments well fits with the possible use of iPS-derived ovarian cells (obtained from recipient dermal fibroblasts) to repopulated decellularized ovarian tissue from a xenogeneic source or from human cadaveric organ donors [39]. Although, these results are still preliminary, they pave the way toward further research that will use primary ovarian cell populations for bioscaffold re-seeding, with interesting implications in the field of reproductive biology and biotechnology [55]. In particular, this novel decellularization protocol, that combines physical and chemical methods and preserves shape, architecture, and ECM of the original organ, may represent the first step toward the obtainment of whole-ovary bioscaffolds that may constitute a suitable niche for ex vivo culture of ovarian cells and follicles, as well as a promising tool for the reconstruction of a bioengineered ovary.

Acknowledgments The Laboratory of Biomedical Embryology is a member of the COST Action CA16119 In vitro 3-D total cell guidance and fitness (CellFit). SEM analysis was carried out at NOLIMITS, an advanced imaging facility established by the Università degli Studi di Milano.

Funding information This work was funded by Carraresi Foundation and PSR2017.

Compliance with ethical standards

This article does not contain any studies with animals performed by any of the authors.

Conflict of interest The authors declare that they have no conflict of interest.

References

1. Hewlett M, Mahalingaiah S. Update on primary ovarian insufficiency. Curr Opin Endocrinol Diabetes Obes. 2015;22:483–9.
2. Qin Y, Jiao X, Simpson JL, Chen Z-J. Genetics of primary ovarian insufficiency: new developments and opportunities. Hum Reprod Update. 2015;21:787–808.
3. Gandolfi F, Ghiringhelli M, Brevini TAL, Gandolfi F, Ghiringhelli M, Brevini TAL. Bioengineering the ovary to preserve and reestablish female fertility. Anim Reprod. 2019;16:45–51.
4. Trinh X-B, Peeters F, Tjalma WAA. The thoughts of breast cancer survivors regarding the need for starting hormone replacement therapy. Eur J Obstet Gynecol Reprod Biol. 2006;124:250–3.
5. Yalcinkaya TM, Sittadjody S, Opara EC. Scientific principles of regenerative medicine and their application in the female reproductive system. Maturitas. 2014;77:12–9.
6. Sadri-Ardekani H, Atala A. Regenerative medicine for the treatment of reproductive system disorders: current and potential options. Adv Drug Deliv Rev. 2015;82–83:145–52.
7. Siegel RL, Miller KD, Jemal A. Cancer statistics, 2019. CA Cancer J Clin. 2019;69:7–34.
8. Vajta G, Kuwayama M. Improving cryopreservation systems. Theriogenology. 2006;65:236–44.
9. Wong KM, Mastenbroek S, Repping S. Cryopreservation of human embryos and its contribution to in vitro fertilization success rates. Fertil Steril. 2014;102:19–26.
10. Sparks A. Human embryo cryopreservation—methods, timing, and other considerations for optimizing an embryo cryopreservation program. Semin Reprod Med. 2015;33:128–44.
11. Chen C. Pregnancy after human oocyte cryopreservation. Lancet. 1986;327:884–6.
12. Westphal LM, Massie JAM, Lentscher JA. Embryo and oocyte banking. Textb Oncofertility Res Pract. 2019. p. 71–9.
13. Porcu E. Oocyte freezing. Semin Reprod Med. 2001;19:221–30.
14. Davis VJ. Female gamete preservation. Cancer. 2006;107:1690–4.
15. Gook DA, Edgar DH. Cryopreservation of female reproductive potential. Best Pract Res Clin Obstet Gynaecol. 2019;55:23–36.
16. Donnez J, Dolmans M-M, Pellicer A, Diaz-Garcia C, Sanchez Serrano M, Schmidt KT, et al. Restoration of ovarian activity and pregnancy after transplantation of cryopreserved ovarian tissue: a review of 60 cases of reimplantation. Fertil Steril. 2013;99:1503–13.
17. Donnez J, Dolmans M-M. Fertility preservation in women. Nat Rev Endocrinol. 2013;9:735–49.
18. Suzuki N, Yoshioka N, Takae S, Sugishita Y, Tamura M, Hashimoto S, et al. Successful fertility preservation following ovarian tissue vitrification in patients with primary ovarian insufficiency. Hum Reprod. 2015;30:608–15.
19. Maffei S, Hanenberg M, Pennarossa G, Silva JRV, Brevini TAL, Arav A, et al. Direct comparative analysis of conventional and directional freezing for the cryopreservation of whole ovaries. Fertil Steril. 2013;100:1122–31.
20. Maffei S, Pennarossa G, Brevini TAL, Arav A, Gandolfi F. Beneficial effect of directional freezing on in vitro viability of cryopreserved sheep whole ovaries and ovarian cortical slices. Hum Reprod. 2014;29:114–24.
21. Moffa F, Biacchiardi CP, Fagioli F, Biasin E, Revelli A, Massobrio M, et al. Ovarian tissue cryostorage and grafting: an option to preserve fertility in pediatric patients with malignancies. Pediatr Hematol Oncol. 2007;24:29–44.
22. Hutt KJ, Albertini DF. An oocentric view of folliculogenesis and embryogenesis. Reprod BioMed Online. 2007;14:758–64.
23. Meirow D, Hardan I, Dor J, Fridman E, Elizur S, Ra'anani H, et al. Searching for evidence of disease and malignant cell contamination in ovarian tissue stored from hematologic cancer patients. Hum Reprod. 2008;23:1007–13.
24. Dolmans MM, Marinescu C, Saussoy P, Van Langendonckt A, Amorim C, Donnez J. Reimplantation of cryopreserved ovarian tissue from patients with acute lymphoblastic leukemia is potentially unsafe. Blood. 2010;116:2908–14.
25. Greve T, Clasen-Linde E, Andersen MT, Andersen MK, Sørensen SD, Rosendahl M, et al. Cryopreserved ovarian cortex from patients with leukemia in complete remission contains no apparent viable malignant cells. Blood. 2012;120:4311–6.
26. Gilpin A, Yang Y. Decellularization strategies for regenerative medicine: from processing techniques to applications. Biomed Res Int. 2017;2017:9831534.

27. Porzionato A, Stocco E, Barbon S, Grandi F, Macchi V, De Caro R. Tissue-engineered grafts from human decellularized extracellular matrices: a systematic review and future perspectives. Int J Mol Sci. 2018;19.
28. Rajabi-Zeleti S, Jalili-Firoozinezhad S, Azarnia M, Khayyatan F, Vahdat S, Nikeghbalian S, et al. The behavior of cardiac progenitor cells on macroporous pericardium-derived scaffolds. Biomaterials. 2014;35:970–82.
29. Lecht S, Stabler CT, Rylander AL, Chiaverelli R, Schulman ES, Marcinkiewicz C, et al. Enhanced reseeding of decellularized rodent lungs with mouse embryonic stem cells. Biomaterials. 2014;35:3252–62.
30. Lee H, Han W, Kim H, Ha D-H, Jang J, Kim BS, et al. Development of liver decellularized extracellular matrix bioink for three-dimensional cell printing-based liver tissue engineering. Biomacromolecules. 2017;18:1229–37.
31. Yu YL, Shao YK, Ding YQ, Lin KZ, Chen B, Zhang HZ, et al. Decellularized kidney scaffold-mediated renal regeneration. Biomaterials. 2014;35:6822–8.
32. Aulino P, Costa A, Chiaravalloti E, Perniconi B, Adamo S, Coletti D, et al. Muscle extracellular matrix scaffold is a multipotent environment. Int J Med Sci. 2015;12:336–40.
33. Baiguera S, Del Gaudio C, Kuevda E, Gonfiotti A, Bianco A, Macchiarini P. Dynamic decellularization and cross-linking of rat tracheal matrix. Biomaterials. 2014;35:6344–50.
34. Sjöqvist S, Jungebluth P, Lim ML, Haag JC, Gustafsson Y, Lemon G, et al. Experimental orthotopic transplantation of a tissue-engineered oesophagus in rats. Nat Commun. 2014;5:3562.
35. Singh A, Bivalacqua TJ, Sopko N. Urinary tissue engineering: challenges and opportunities. Sex Med Rev. 2018;6:35–44.
36. Kajbafzadeh A-M, Khorramirouz R, Kameli SM, Hashemi J, Bagheri A. Decellularization of human internal mammary artery: biomechanical properties and histopathological evaluation. Biores Open Access. 2017;6:74–84.
37. Zhang J-K, Du R-X, Zhang L, Li Y-N, Zhang M-L, Zhao S, et al. A new material for tissue engineered vagina reconstruction: Acellular porcine vagina matrix. J Biomed Mater Res Part A. 2017;105:1949–59.
38. Laronda MM, Rutz AL, Xiao S, Whelan KA, Duncan FE, Roth EW, et al. A bioprosthetic ovary created using 3D printed microporous scaffolds restores ovarian function in sterilized mice. Nat Commun. 2017;8:15261.
39. Laronda MM, Jakus AE, Whelan KA, Wertheim JA, Shah RN, Woodruff TK. Initiation of puberty in mice following decellularized ovary transplant. Biomaterials. 2015;50:20–9.
40. Pors SE, Ramløse M, Nikiforov D, Lundsgaard K, Cheng J, Andersen CY, et al. Initial steps in reconstruction of the human ovary: survival of pre-antral stage follicles in a decellularized human ovarian scaffold. Hum Reprod. 2019;34:1523–35.
41. Liu W-Y, Lin S-G, Zhuo R-Y, Xie Y-Y, Pan W, Lin X-F, et al. Xenogeneic decellularized scaffold: a novel platform for ovary regeneration. Tissue Eng Part C Methods. 2017;23:61–71.
42. Hassanpour A, Talaei-Khozani T, Kargar-Abarghouei E, Razban V, Vojdani Z. Decellularized human ovarian scaffold based on a sodium lauryl ester sulfate (SLES)-treated protocol, as a natural three-dimensional scaffold for construction of bioengineered ovaries. Stem Cell Res Ther. 2018;9:252.
43. Eivazkhani F, Abtahi NS, Tavana S, Mirzaeian L, Abedi F, Ebrahimi B, et al. Evaluating two ovarian decellularization methods in three species. Mater Sci Eng C. 2019;102:670–82.
44. Alshaikh AB, Padma AM, Dehlin M, Akouri R, Song MJ, Brännström M, et al. Decellularization of the mouse ovary: comparison of different scaffold generation protocols for future ovarian bioengineering. J Ovarian Res. 2019;12:58.
45. Bondioli K, Ramsoondar J, Williams B, Costa C, Fodor W. Cloned pigs generated from cultured skin fibroblasts derived from a H-transferase transgenic boar. Mol Reprod Dev. 2001;60:189–95.
46. Oktem O, Oktay K. The role of extracellular matrix and activin-A in in vitro growth and survival of murine preantral follicles. Reprod Sci. 2007;14:358–66.
47. Oktay K, Karlikaya G, Akman O, Ojakian GK, Oktay M. Interaction of extracellular matrix and activin-A in the initiation of follicle growth in the mouse ovary. Biol Reprod. 2000;63:457–61.
48. Laronda MM. Engineering a bioprosthetic ovary for fertility and hormone restoration. Theriogenology. 2020;S0093-691X(20):30027–3.
49. O'Neill JD, Anfang R, Anandappa A, Costa J, Javidfar J, Wobma HM, et al. Decellularization of human and porcine lung tissues for pulmonary tissue engineering. Ann Thorac Surg. 2013;96:1046–56.
50. Zhou J, Fritze O, Schleicher M, Wendel H-P, Schenke-Layland K, Harasztosi C, et al. Impact of heart valve decellularization on 3-D ultrastructure, immunogenicity and thrombogenicity. Biomaterials. 2010;31:2549–54.
51. Uygun BE, Soto-Gutierrez A, Yagi H, Izamis M-L, Guzzardi MA, Shulman C, et al. Organ reengineering through development of a transplantable recellularized liver graft using decellularized liver matrix. Nat Med. 2010;16:814–20.
52. Henning NF, LeDuc RD, Even KA, Laronda MM. Proteomic analyses of decellularized porcine ovaries identified new matrisome proteins and spatial differences across and within ovarian compartments. Sci Rep. 2019;9:20001.
53. Morris AH, Stamer DK, Kyriakides TR. The host response to naturally-derived extracellular matrix biomaterials. Semin Immunol. 2017;29:72–91.
54. Laronda MM, Burdette JE, Kim J, Woodruff TK. Recreating the female reproductive tract in vitro using iPSC technology in a linked microfluidics environment. Stem Cell Res Ther. 2013;4:S13.
55. Brevini TAL, Pennarossa G, Gandolfi F. A 3D approach to reproduction. Theriogenology. 2020;S0093-691X(20):30026–1.